Developmental Biology 385 (2014) 316–327

Contents lists available at ScienceDirect

Developmental Biology

journal homepage: www.elsevier.com/locate/developmentalbiology

Gβ1 controls collective cell migration by regulating the protrusive activity of leader cells in the posterior lateral line primordium

Hui Xu [a], Ding Ye [a], Martine Behra [c], Shawn Burgess [d], Songhai Chen [b], Fang Lin [a,*]

[a] Department of Anatomy and Cell Biology, Carver College of Medicine, University of Iowa, USA
[b] Department of Pharmacology, Carver College of Medicine, University of Iowa, USA
[c] Department of Anatomy and Neurobiology, University of Puerto Rico, USA
[d] Genome Technology Branch, NHGRI/NIH, Bethesda, MD, USA

ARTICLE INFO

Article history:
Received 16 August 2013
Received in revised form
16 October 2013
Accepted 27 October 2013
Available online 4 November 2013

Keywords:
Zebrafish
G protein
Gβ1
Posterior lateral line primordium
Cell migration

ABSTRACT

Collective cell migration is critical for normal development, tissue repair and cancer metastasis. Migration of the posterior lateral line primordium (pLLP) generates the zebrafish sensory organs (neuromasts, NMs). This migration is promoted by the leader cells at the leading edge of the pLLP, which express the G protein-coupled chemokine receptor Cxcr4b and respond to the chemokine Cxcl12a. However, the mechanism by which Cxc112a/Cxcr4b signaling regulates pLLP migration remains unclear. Here we report that signal transduction by the heterotrimeric G protein subunit Gβ1 is essential for proper pLLP migration. Although both Gβ1 and Gβ4 are expressed in the pLLP and NMs, depletion of Gβ1 but not Gβ4 resulted in an arrest of pLLP migration. In embryos deficient for Gβ1, the pLLP cells migrated in an uncoordinated fashion and were unable to extend protrusions at the leading front, phenocopying those in embryos deficient for Cxcl12a or Cxcr4b. A transplantation assay showed that, like Cxcr4b, Gβ1 is required only in the leader cells of the pLLP. Analysis of F-actin dynamics in the pLLP revealed that whereas wild-type leader cells display extensive actin polymerization in the direction of pLLP migration, counterparts defective for Gβ1, Cxcr4b or Cxcl12a do not. Finally, synergy experiments revealed that Gβ1 and Cxcr4b interact genetically in regulating pLLP migration. Collectively, our data indicate that Gβ1 controls migration of the pLLP, likely by acting downstream of the Cxcl12a/Cxcr4b signaling. This study also provides compelling evidence for functional specificity among Gβ isoforms *in vivo*.

Introduction

Collective cell migration—tightly coordinated movement of a group of cells—is an important strategy that cells utilize not only during development, but also during tissue invasion and metastasis in the context of cancer (Friedl and Gilmour, 2009; Lecaudey and Gilmour, 2006; Rorth, 2009). Elucidating the mechanisms that underlie this form of migration will be critical to understanding both normal and aberrant morphogenesis. A key feature of collective migration is that cell–cell contact and communication are maintained. As in the case of single-cell migration, collective migration depends on polarized protrusive activities of cells at the leading edge. However, unlike single cells, the grouped cells do not establish their polarity individually. Rather, their polarity is established by the formation of two regions that are morphologically and functionally distinct: the leading and trailing regions of the cluster. Within the leading region, the so-called leader cells have free edges to expose to the extracellular environment. Thus, they can receive migration cues, in response to which they generate a pulling force that directs the migration of the entire cell cluster (Caussinus et al., 2008; De Smet et al., 2009; Haas and Gilmour, 2006; Wolf et al., 2007). Although significant progress has been made toward understanding the process of collective migration, the mechanisms whereby the leader cells respond to external cues remain to be fully elucidated.

The zebrafish lateral line (LL) is an excellent model for studying collective cell migration, due to the genetic tractability of zebrafish and the accessibility of this structure to *in vivo* imaging (Dambly-Chaudiere et al., 2003; Ghysen and Dambly-Chaudiere, 2004). It is a sensory system that detects water currents and consists of neuromasts (NMs), mechanosensory organs located on the animal's surface (Dambly-Chaudiere et al., 2003; Ghysen and Dambly-Chaudiere, 2007). Posterior NMs located in the trunk and the tail regions are produced by the posterior LL primordium (pLLP), a cluster of 100 cells that migrate collectively from the otic vesicle to the tip of the tail, along the myoseptum (Ghysen and Dambly-Chaudiere, 2007). The pLLP is morphologically patterned. Cells in the leading region display a mesenchymal shape and actively extend filopodia and pseudopodia in response to external cues. In contrast, cells in the trailing region are organized into epithelial rosette-like structures (pro-neuromasts) that separate from the cluster periodically and are deposited along the trunk, where they develop into functional NMs (Valentin et al., 2007).

* Corresponding author. Fax: +1 319 335 7198.
E-mail addresses: fang-lin@uiowa.edu, fanglin68@gmail.com (F. Lin).

0012-1606/$ - see front matter © 2013 Elsevier Inc. All rights reserved.
http://dx.doi.org/10.1016/j.ydbio.2013.10.027

Thus, LL development involves a complex series of coordinated cellular processes (i.e., morphogenesis, collective cell migration, proliferation, and differentiation) that require interactions among a network of signaling pathways (Aman and Piotrowski, 2009; Ghysen and Dambly-Chaudiere, 2007; Ma and Raible, 2009).

Whereas NM deposition is controlled by fibroblast growth-factor (FGF) activity orchestrated by the Wnt signaling pathway (Aman and Piotrowski, 2008; Lecaudey et al., 2008; Nechiporuk and Raible, 2008), pLLP migration is regulated by the chemokine Cxcl12a (Sdf1a) and its cognate receptors, Cxcr4b and Cxcr7b (Dambly-Chaudiere et al., 2007; David et al., 2002; Haas and Gilmour, 2006; Li et al., 2004; Valentin et al., 2007). Embryos depleted of Cxcl12a, Cxcr4b or Cxcr7b exhibit severe disruption of pLLP migration, resulting in either the failure or premature termination of pLLP migration (Dambly-Chaudiere et al., 2007; David et al., 2002; Haas and Gilmour, 2006; Li et al., 2004; Valentin et al., 2007). *cxcl12a* is expressed in cells along the myoseptum, forming a track that mirrors the path of pLLP migration. Cxcl12a has thus been proposed to guide pLLP migration (Dambly-Chaudiere et al., 2007; David et al., 2002).

It has also been established that asymmetric and complementary expression of the Cxcr4b and Cxcr7b receptors within the pLLP is essential for the migration of this tissue, with *cxcr4b* expressed in the leading region, and *cxcr7b* in the trailing region (Dambly-Chaudiere et al., 2007; Valentin et al., 2007). Cxcr4b in the leader cells (i.e., those that are present at the very tip of the pLLP, and are exposed to extracellular signals) triggers chemotaxis in response to Cxcl12a (Haas and Gilmour, 2006; Valentin et al., 2007). Cxcr7b in the trailing region antagonizes Cxcr4b function, presumably by internalizing Cxcl12a and thereby generating a local concentration gradient of the ligand (Dambly-Chaudiere et al., 2007; Ghysen and Dambly-Chaudiere, 2007; Valentin et al., 2007). However, a more direct role for Cxcr7 in controlling cell–cell interactions in the trailing region of the pLLP has been also reported (Valentin et al., 2007).

How Cxcr4b activates downstream signaling to promote pLLP migration remains unknown. This protein is a member of the G protein-coupled receptor (GPCR) family, whose members are known to control cellular processes by activating heterotrimeric G protein complexes (Thelen, 2001). The latter consist of α, β and γ subunits. Upon ligand stimulation, the Gα subunit and Gβγ dimer dissociate from one another, and both are capable of triggering downstream signaling. Gβγ is functional only in dimeric form, although its signaling properties are mediated primarily by interactions between Gβ and downstream effectors (Dupre et al., 2009; Smrcka, 2008). Previous studies in leukocytes and *Dictostelium* indicate that in the context of chemotaxis Cxcr4 signals mainly through Gβγ, following its separation from the associated Gαi protein (Peracino et al., 1998; Rickert et al., 2000).

In this study we investigated the function of Gβγ signaling in Cxcr4b-mediated pLLP migration, by analyzing expression, phenotypes and synergy. We show that: the Gβ1 and Gβ4 isoforms are expressed in the LL, but only Gβ1 is required for pLLP migration; Gβ1 is required specifically in the leader cells; Gβ1 interacts with Cxcr4b genetically to regulate migration; and Cxcr4b/Gβ1 signaling regulates F-actin dynamics and the formation of protrusions in the leading cells. Taken together, these findings indicate that Gβ1 controls the function of the leader cells during pLLP migration, and suggest that it acts downstream of Cxcl12a/Cxcr4b signaling.

Materials and methods

Zebrafish strains

WT (Tubingen, Tubingen/AB), transgenic *Tg*(*-8.0cldnb*:*lynEGFP*) (Haas and Gilmour, 2006), *Tg*(*ET20*:*GFP*) (Parinov et al., 2004), *Tg*(*SCM1*:*GFP*) (Behra et al., 2009), and *ody*$^{(-/-)}$ mutant (Knaut et al., 2003) strains of zebrafish were used in this study. Zebrafish were maintained as described previously (Xu et al., 2011). Embryos were obtained through natural mating and staged according to morphology or hours post fertilization (hpf) at 28.5 °C, as described previously (Kimmel et al., 1995).

Generation of the Tg(-135bpcxcr4b:lifeact-RFP) transgenic line

We expressed Lifeact-RFP specifically in the LL using a 139 bp *cxcr4b* promoter previously shown to drive the expression of target genes specifically in the pLL (Gamba et al., 2010). We generated the *-135bpcxcr4b*:*lifeact-RFP* transgenic construct using the MultiSite Gateway system (Life Technologies, Carlsbad, CA). To generate a 5′ entry construct, we removed the last 4 bp of the C-terminus of the 139 bp *cxcr4b* promoter to maintain the correct reading frame of a middle entry gene, *lifeact-RFP* (Berepiki et al., 2010) following Gateway recombination. The 5′ entry plasmid (containing 135 bp *cxcr4b* promoter) and the middle entry plasmid (containing the coding sequence of *lifeact-RFP*) were cloned into a destination vector (pDestTol2CG2) (Kwan et al., 2007) using the Tol2-based Gateway system. Thirty picograms of the transgene plasmid DNA was co-injected with 30 pg of transposase RNA into the cytoplasm of embryos at the one-cell stage. Injected embryos in which GFP expression was present in the heart at 24 hpf were raised, and stable transgenic lines in which the Lifeact-RFP was expressed within the LL were generated.

Morpholino (MO) injection

MOs (obtained from Gene Tools, LLC) were injected into embryos at the one-cell stage, at the indicated doses (the nucleotides that target the ATG initiation codon are underlined). In the cases of all MO injections, 2 ng of *p53* MO was co-injected to reduce the general apoptosis triggered by the MOs (Robu et al., 2007). Two sets of MOs targeting *gnb1* and *gnb4* were used. For *gnb1* (*gnb1a* and *gnb1b*): the first set of MOs inhibits translation, as previously validated (Xu et al., 2012), and the individual MOs are referred as *gnb1a* MO1 (2 ng, 5′-GAGTTCGCTCATTTTCTTCTGCTTC-3′) and *gnb1b* MO1 (2 ng, 5′-CTGGTCCAGTTCACTCATTTTCCTC-3′), respectively; the second set of MOs inhibits *gnb1a* translation and blocks *gnb1b* splicing, as previously validated (Hippe et al., 2009), and the individual MOs are referred as *gnb1a* MO2 (3 ng, 5′-CTGGTCGAGTTCGCTCATTTTCTTC-3′) and *gnb1b* MO2 (8 ng, 5′-AATTAGGTGGTTACCTGTGATAGT-3′, targets the splice site at the junction between the 1st exon and intron). For *gnb4* (*gnb4a* and *gnb4b*), the first set of MOs block translation, as previously validated (Xu et al., 2012), and the individual MOs are referred as *gnb4a* MO1 (4 ng, 5′-CCGCAACTGCTC CAGCTCACTCATG-3′) and *gnb4b* MO1 (4 ng, 5′-GACGCAACTGCTCCAACTCACTCAT-3′); the second set of MOs targets the splicing of *gnb4a* and *gnb4b* and the individual MOs are referred as *gnb4a* MO2 (8 ng, 5′-GCATCCTGCAATGGGAACAGCAGCA-3′, targets the splice site at the junction between the 2nd intron and the 3rd exon) and *gnb4b* MO2 (8 ng, 5′-TGTTACGGAGTCACCCTTACCCGGA-3′, targets the splice site at the junction between the 2nd exon and intron). RT-PCR performed on RNA isolated from 28-hpf embryos revealed that embryos injected with *gnb4a* MO2 or *gnb4b* MO2 produced smaller amplicons than uninjected control embryos (Fig. S2F), confirming that the MOs used disrupted normal splicing.

Whole-mount in situ hybridization

Sense and antisense RNA probes were synthesized by *in vitro* transcription. Whole-mount in situ hybridization was performed as described previously (Lin et al., 2005; Thisse and Thisse, 2008).

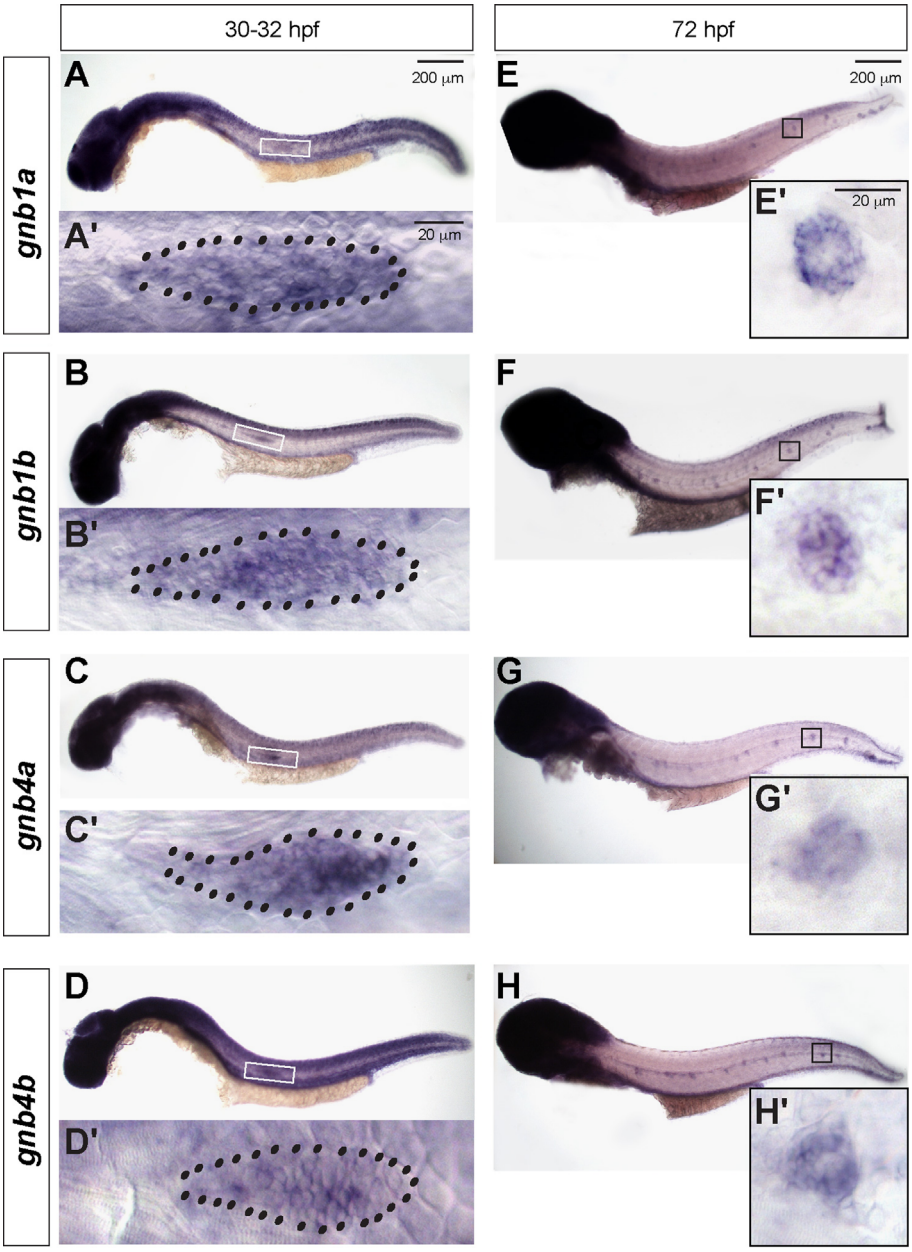

Fig. 1. *gnb1* (*a* and *b*) and *gnb4* (*a* and *b*) are expressed in the migrating pLLP and in deposited NMs. Transcripts of the indicated genes were detected by whole-mount *in situ* hybridization. (A–D) Embryos at 30–32 hpf and (A'–D') High-magnification images of the boxed areas in A–D. Dots outline the pLLP. (E–H) Embryos at 72 hpf and (E'–H') high magnification images of NMs in the boxed areas in E–H. All images are lateral views with anterior to the left. hpf: hours post fertilization.

Probes encoding the *gnb1* and *gnb4* genes were described previously (Xu et al., 2011). Other RNA probes used in this study include: *eya1* (Nica et al., 2006), *cxcr4b* and *cxcl12a* (Doitsidou et al., 2002).

Whole-mount immunofluorescence staining

Embryos were fixed overnight at the indicated stages, in 4% PFA/PBS/4% sucrose at 4 °C. Whole-mount immunohistochemistry was performed as described previously (Lin et al., 2005). The following antibodies were used: pan-Gβ (1:200, Santa Cruz Biotechnology, Santa Cruz, CA) and Gβ1 (1:200, GeneTex, Irvine, CA).

Western blotting

Embryos were manually de-yolked and homogenized in lysis buffer (2 × RIPA buffer) containing protease inhibitors (1 g/ml of aprotinin, leupeptin and pepstatin, 1 mM PMSF 1 mM), and equal amounts of protein were used for Western blot analysis as described previously (Lin et al., 2009). The following primary antibodies were used: pan-Gβ (1:5000, Santa Cruz Biotechnology, Santa Cruz, CA), zebrafish Gβ1 (1:5000, GeneTex, Irvine, CA), and α-Tubulin (a loading control; 1:10,000, Sigma, St. Louis, MO). Immunoblots were analyzed using an Odyssey infrared imaging system (LI-COR Biosciences, Lincoln, NE).

Transplantation

Donor embryos injected with 0.3% rhodamine dextran (Invitrogen Molecular Probes) at the 1-cell stage were allowed to develop to the sphere stage. Approximately 20–30 donor cells were transplanted into the presumptive placodal domain of *Tg* (*-8.0cldnb*:*lynEGFP*) host embryos at shield stage, as described previously (Nechiporuk and Raible, 2008). Host embryos were screened for the presence of donor cells in the pLLP at 24 hpf.

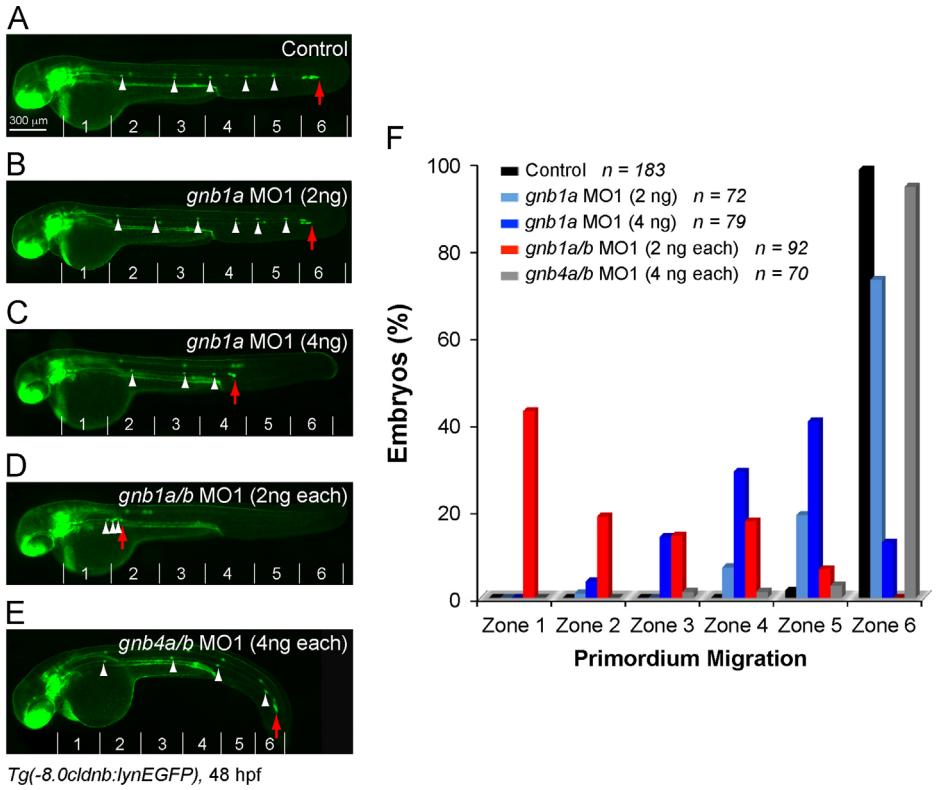

Fig. 2. Gβ1, but not Gβ4, is required for migration of the pLLP. (A–E) Epifluorescence images of 48-hpf *Tg(-8.0cldnb:lynEGFP)* control embryos (A), embryos injected with MOs targeting *gnb1a* (B, C), *gnb1a/b* (D) or *gnb4a/b* (E). All images are lateral views with anterior to the left. White arrowheads, NMs. The embryo was subdivided into six equal sections (zones 1–6) from the ear to the tip of the tail. (F) Quantification of pLLP migration relative to the position of the posterior-most deposited NM (red arrows in A–E). The number of animals/injection is indicated.

TUNEL assay

Tg(-8.0cldnb:lynEGFP) embryos at 30–32 hpf were fixed overnight in 4% PFA at 4 °C. Whole-mount TUNEL assay was performed using an apoptosis detection kit (ApopTag Red *in situ* apoptosis Detection Kit, Millipore). The EGFP-expressing pLLP was analyzed for presence of Rhodamine-labeled apoptotic cells (red).

Microscopy, time-lapse imaging and analysis

Live embryos were mounted in 1% methylcellulose and photographed using a Leica DMI 6000 microscope with a 5 × /NA 0.15 objective. Fixed embryos were mounted in 75% glycerol/PBS and photographed using a Leica M165FC stereofluorescence microscope and a Leica DFC290 color digital camera. For time-lapse imaging, embryos were anesthetized in 0.01% tricaine and embedded in 1% low melting-point agarose. Epifluorescence time-lapse images were taken on a Leica DMI 6000 microscope using the 5 × /NA 0.15 or 10 × /NA 0.30 objective; samples were placed on a stage heated to 28.5 °C. Confocal imaging was performed using a laser-scanning confocal inverted microscope (LSM700, Carl Zeiss, Inc.) with a 20 × /NA 0.8 air or 40 × /NA 1.3 oil objective. For confocal time-lapse imaging, 3–4 z-stacks representing a total thickness of 10 μm were captured and are presented as maximum projections in the figures. To determine the relationships between actin bursts and protrusion formation in the leading cells of the pLLP, kymograph analyses (using the kymograph plugin for Image J) were performed on the protruding region of the migrating pLLP. The ROI manager was used to ensure that the signals measured in the RFP and GFP channels were from the same region. To quantify the average LifeactRFP intensity in the trailing region where the rosettes are located, we performed confocal time-lapse experiments covering the whole migrating pLLP (20 ×). Projections of Z-stack images were generated using the ImageJ software, and at least four random areas outside the rosettes were chosen per embryo to determine the mean gray value. All time-lapse images were first analyzed using the Metamorph or ImageJ software, and then further compiled and edited using Adobe Photoshop® and Illustrator software. Scale bars are provided in all figures.

Statistical analysis

Data were compiled from at least two independent experiments and are presented as the mean ± SEM. The following statistical analyses were used: Chi-Square analyses for assessing differences in pLLP distribution (Figs. 2F and 7E), two-way analysis of variance (ANOVA) for assessing changes in migration speed (Fig. 3E), and student's *t*-test with unequal variance for assessing differences in the number of protrusions and length of the filopodia (Figs. 5 and S6). Statistical significance was set at $p \leq 0.05$. The number of embryos analyzed in each experiment is indicated in the figures.

Results

Gβ1 and Gβ4 are expressed in the pLLP and NMs

In investigating the functions of Gβγ signaling in pLLP development, we focused on Gβ, as there are fewer isoforms than for Gγ, making targeting easier. We previously identified five Gβ isoforms (nine members, of which all except Gβ2 are duplicated) in the zebrafish genome. Among the encoding genes, those for the Gβ1 and Gβ4 isoforms (*gnb1a*, *gnb1b*, *gnb4a*, and *gnb4b*) are maternally and ubiquitously expressed during gastrulation (Xu et al., 2012).

In this study, we found that their expression continues throughout the embryo from 30–48 hours post fertilization (hpf), particularly in the anterior region of embryo (Fig. 1). Notably, they are also expressed in the migrating pLLP at 32 hpf (Fig. 1A–D) and in the deposited NMs at 72 hpf (Fig. 1E–H). The genes that encode Gβ2, Gβ3 and Gβ5 are not expressed until 24–48 hpf, and their expression during this period is limited to the central nervous system, cranial ganglion, epiphysis, eye and retina (not shown) (Thisse and Thisse, 2004). Thus, only Gβ1 and Gβ4 are candidates for involvement in development of the LL.

Gβ1, but not Gβ4, is essential for pLLP migration

To investigate the functions of Gβ1 and Gβ4 during pLLP migration, we inhibited their expression using previously validated antisense morpholino oligonucleotides (MOs, in this case MO1) (Xu et al., 2012). Western blotting using an antibody that specifically recognizes zebrafish Gβ1 (both the Gβ1a and Gβ1b isoforms) confirmed that injection of MOs targeting both *gnb1a* and *gnb1b* (*gnb1a*/*b* MO1) led to 81% reduction of the Gβ1 expression in 24-hpf embryos (Fig. S1A, left panel). Immunofluorescence analysis with the same antibody showed that expression in the migrating pLLP was nearly eliminated (Fig. S1B, middle panel). To examine the effects of the *gnb4* MO1, we used a pan-Gβ antibody that recognizes all Gβ isoforms except Gβ5, since a specific antibody for Gβ4 is not yet available (Lin et al., 2009). Western blotting showed that total Gβ protein was reduced by 60% and 54% in *gnb1a*/*b* MO1 and *gnb4a*/*b* MO1 injected-embryos, respectively, at 24 hpf (Fig. S1A, right panel). Similarly, immunofluorescence analysis of the migrating pLLP showed that total Gβ expression was significantly reduced in embryos injected with MOs targeting either *gnb1a*/*b* or *gnb4a*/*b*, but that a substantial amount of Gβ remained in the pLLP when only one Gβ isoform was inhibited (Fig. S1C). Additionally, Gβ1 expression in the pLLP of *gnb4a*/*b* MO1-injected embryos was similar to that in uninjected control embryos (Fig. S1B, bottom panel), suggesting that inhibiting Gβ4 expression did not affect the Gβ1 expression in the pLLP. These data indicate that the MOs used in this study efficiently suppress expression of the corresponding Gβ isoforms in zebrafish embryos, including in the migrating pLLP, and that the inhibition of one Gβ isoform does not significantly affect the expression of others.

We assessed the effects of inhibiting Gβ expression on development of the LL using the *Tg*(*-8.0cldnb*:*lynEGFP*) transgenic line, in which membrane-bound GFP is expressed in the LL (Haas and Gilmour, 2006). In control (uninjected) embryos at 48 hpf, the pLLP reached the end of the tail (Fig. 2A, red arrow; F, zone 6) and 5–6 NMs were deposited along the trunk (Fig. 2A, white arrowheads). In contrast, in embryos injected with MOs against either *gnb1a* or *gnb1b*, the pLLP failed to migrate to the tail and both the pLLP and NMs were limited to anterior regions (Fig. 2). These findings are consistent with an impairment of pLLP migration. Both the severity and penetrance of these pLLP migration defects increased with the dose of MO injected (Fig. 2B, C, and F). To quantify the pLLP migration defects, we divided the region from the ear to the tip of the tail into six equal sections (Fig. 2A–E), with zone 1 closest to the ear and zone 6 at the tip of the tail (Valentin et al., 2007). We found that in embryos injected with a low dose of *gnb1a* MO1 (2 ng), the pLLP migrated to zone 6 in 73% of embryos ($n=72$), and reached zones 4 and 5 in the remaining embryos (Fig. 2B and F). In embryos injected with a higher dose of the same MO (4 ng), the pLLP reached the tail in only 13% of embryos ($n=79$), but migrated only to approximately the middle of the trunk in the majority of embryos (84%) (Fig. 2C and F). Notably, co-injection of low doses of MOs targeting both *gnb1a* and *gnb1b* (*gnb1a*/*b* MO1, 2 ng each) resulted in a much stronger defect in pLLP migration than did injection of a single MO ($p<0.05$, Chi-square test). In 62% of these embryos ($n=91$), the pLLP showed little migration and reached only the anterior-most region of the trunk (43% in zone 1 and 19% in zone 2) (Fig. 2D and F). Injection of another set of previously validated Gβ1 MOs, i.e., a second MO that targets the translation of *gnb1a* (*gnb1a* MO2), and one that blocks the splicing of *gnb1b* (*gnb1b* MO2) (Hippe et al., 2009) resulted in defects in pLLP migration similar to those obtained using MO1 (Fig. S2B, C, and E vs. Fig. 2D and F). As non-specific cell death resulted from MOs can affect LL development (Aman et al., 2011), we performed the TUNEL analysis in embryos injected with *gnb1a*/*b* MO1 at 30–32 hpf, the point in time at which the pLLP engages in active migration. We found no significant difference in the number of TUNEL-positive cell in the primordium between the control (0.2 ± 0.2, $n=5$) and *gnb1a*/*b* MO-injected embryos (1.2 ± 0.37, $n=5$, $p>0.05$, *t*-test). Thus, the injection of the *gnb1a*/*b* MO did not induce excessive apoptosis in the pLLP, and cell death is unlikely to contribute the stalled migration phenotype observed in Gβ1-deficient pLLP. Intriguingly, embryos injected with high doses of MOs that target the translation and splicing of genes encoding the two isoforms of Gβ4 (4 and

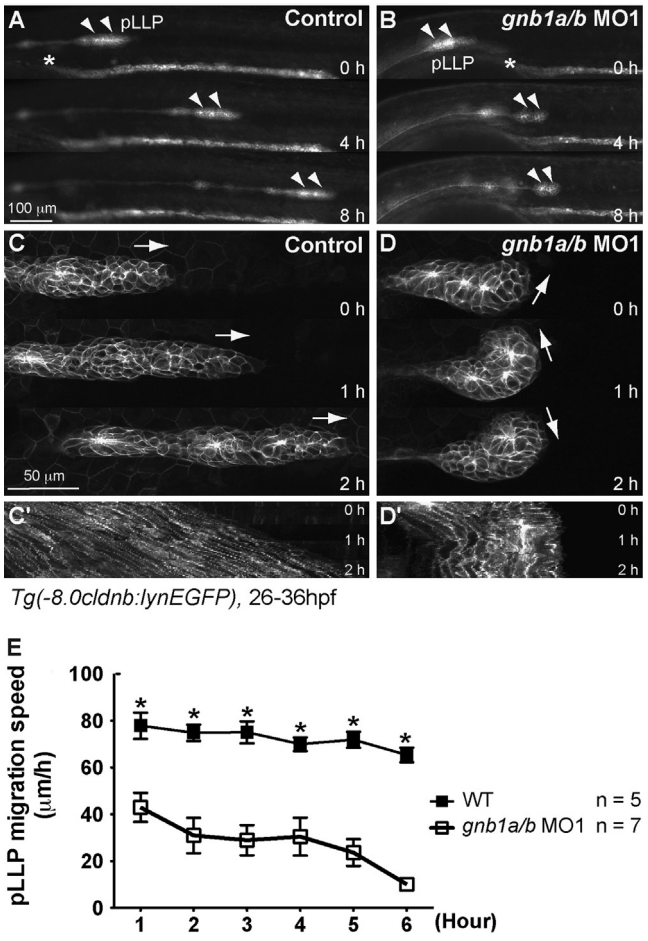

Fig. 3. Gβ1 signaling is required for the coordinated movement of cells within the pLLP. (A, B) Snapshots from 8-h epifluorescence time-lapse movies of control (A) or *gnb1a*/*b* MO1-injected (B). *Tg*(*-8.0cldnb*:*lynEGFP*) embryos, at 28–36 hpf, using a 5 × /NA 0.15 objective (Movies 1 and 2). Lateral views with anterior to the left. Arrowheads, pLLP; *, the anterior-most region of the pronephric duct. (C, D) Snapshots from 2-h confocal time-lapse movies of control (C) or *gnb1a*/*b* MO1-injected (D). *Tg*(*-8.0cldnb*:*lynEGFP*) embryos, starting at 30 hpf, using a 20 × NA 0.8 objective (Movies 3 and 4). The white arrows in C and D indicate the direction of pLLP migration. (C'–D') Kymograph analysis showing the cell traces from the 2-h movies in C and D. (E) Speed of migration (in micrometers per hour) of the pLLP in control or *gnb1a*/*b* MO1-injected embryos recorded for 6 h from 28 to 34 hpf.

8 ng each, respectively, Fig. S2F and G) did not show defects in pLLP migration and NM deposition (Figs. 2E, F and S2D, E, $p > 0.05$, Chi-square test), but rather ventral curvature of the body axis (XH and FL, unpublished data) (Fig. 2E). Taken together, our results indicate that Gβ1, but not Gβ4, is essential for proper migration of the pLLP.

Notably, NMs were deposited in Gβ1 morphants although they were fewer in number and clustered together adjacent to the stalled pLLP (Fig. 2B, D). In addition, the NMs that formed in the pLLP of the *gnb1a/b* MO1-injected embryos had the rosette structure that is critical for their deposition (Figs. 3 and 5). These findings support the notion that pLLP migration and NM deposition are regulated independently (Lecaudey et al., 2008). Furthermore, NM differentiation was not affected in Gβ1 morphants, as revealed by the presence of mantle cells, supporting cells and hair cells at 72 hpf (Fig. S3). Thus, Gβ1 signaling is required for pLLP migration, but not for NM deposition and differentiation.

The pLLP migration defects in Gβ1 morphants resemble those observed in embryos deficient for chemokine signaling (David et al., 2002; Haas and Gilmour, 2006; Li et al., 2004; Valentin et al., 2007). Thus the pLLP migration defects resulting from inhibition of Gβ1 expression could be due to alterations in the expression of chemokine or chemokine receptors. To test this possibility, we performed whole-mount in situ hybridization (ISH) on embryos at 32 hpf. Our results show that although the *gnb1a/b* MO1-injected embryos exhibited migration defects, as demonstrated by the rounded morphology of the pLLP (staining for the pLLP marker *eya1*, Fig. S4A', D') (Kozlowski et al., 2005), the pattern and level of

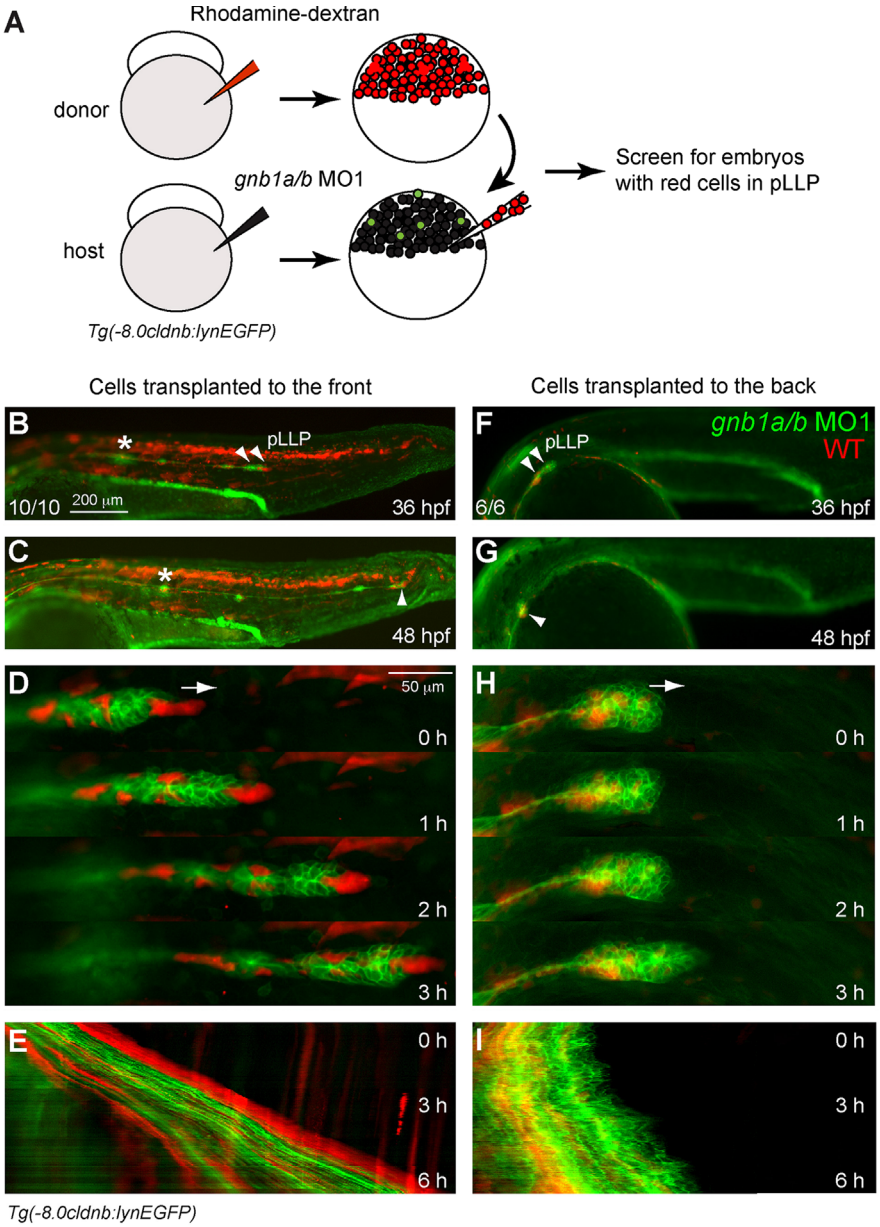

Fig. 4. Gβ1 function in the leading region is required for pLLP migration. (A) Schematic diagram depicting the transplantation procedure. Rhodamine-labeled WT cells (red) were transplanted into *gnb1a/b* MO1-injected *Tg(-8.0cldnb:lynEGFP)* embryos at the shield stage. (B–I) Representative images of Gβ1-depleted embryos in which WT cells were transplanted into the leading region (B–E) or the trailing region (F–I) of the pLLP. (B, F) Embryos at 36 hpf. Arrowheads, pLLP; *, pLLP on contralateral side of embryo. (C, G) Embryos shown in B and F at 48 hpf. Arrowhead, final position of the manipulated pLLP; *, final position of the control pLLP (contralateral side). (D, H) Snapshots from the first 3 h (of the 6 h from 30 to 36 hpf) of time-lapse movies of the embryos shown in B and F. WT cells transplanted into the leading region (C, $n = 10/10$ embryos, Movie 5), but not into the trailing region (E, $n = 6/6$ embryos, Movie 6), rescued the pLLP-migration defects in embryos injected with *gnb1a/b* MO1. (E, I) Kymograph analysis of the 6-h movies partially shown in D and H.

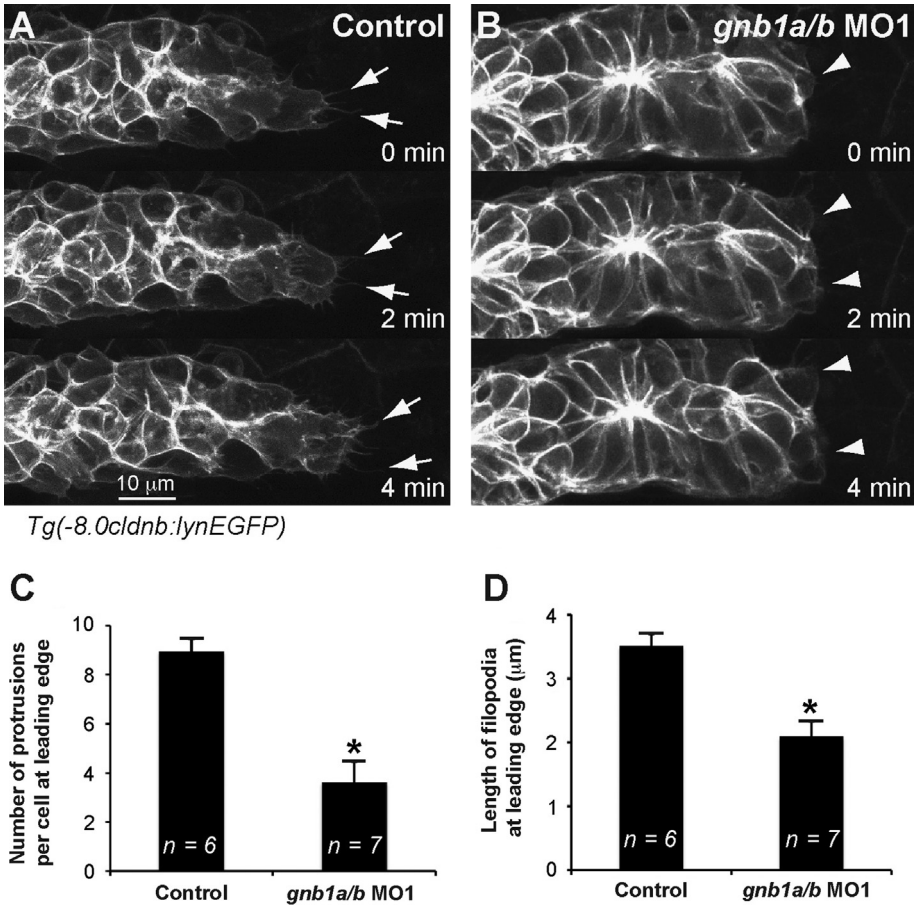

Fig. 5. Gβ1 signaling regulates protrusive activity in the leading region of the pLLP. (A, B) Snapshots of the leading region of the pLLP from 30-min confocal time-lapse movies of control (A) or *gnb1a*/*b* MO1-injected (B) *Tg*(*-8.0cldnb*:*lynEGFP*) embryos, at 30 hpf, using a 40 × /NA 1.3 objective (Movies 7 and 8). White arrows, protrusions at the leading edge of the pLLP. (C, D) Number of protrusions per cell (C) and average length of the filopodia (D) at the leading edge of the pLLP, in control or *gnb1a*/*b* MO1-injected embryos. *, $p < 0.01$ vs. control.

cxcl12a expression were comparable to those in control (uninjected) siblings (Fig. S4A–D). Similarly, the expression patterns of *cxcr4b* and *cxcr7b* were not affected in less polarized pLLP deficient for Gβ1 signaling (Fig. S4B, C, E, and F). Together, these data indicate that the defective pLLP migration in Gβ1 morphants does not result from altered expression of *cxcl12a*, *cxcr4b* or *cxcr7b*.

Gβ1 signaling is required for the coordination of pLLP migration

To investigate how Gβ1 signaling affects pLLP migration, we performed time-lapse experiments at low magnification and imaged the embryos for 8 h starting at 28 hpf. In control embryos, the pLLP migrated caudally at relatively constant speed (72.5 ± 1.8 μm/h), periodically depositing NMs from the trailing region (Fig. 3A and E; Movie 1). In Gβ1 morphants, the pLLP was able to initiate migration, but at significantly reduced speed (43 ± 6 μm/h from 28 to 29 hpf, $p < 0.01$ compared with control, two-way ANOVA, Fig. 3E). The reduction in migration speed was also supported by the observation that the pLLP in the morphants was located at the more anterior region of the trunk as compared to that in control embryos at 28 hpf when the time-lapse experiments were conducted (the anterior-most region of the pronephric duct was marked to illustrate the embryo landmark, Fig. 3A and B). During the following several hours, the pLLP in Gβ1 morphants migrated progressively at slow speed, and eventually stopped completely (Fig. 3B and E, Movie 2).

Supplementary material related to this article can be found online at http://dx.doi.org/10.1016/j.ydbio.2013.10.027.

Previous studies had shown that the cells of the pLLP migrate collectively and in highly synchronous fashion—maintaining their relative positions, and migrating at the same velocity and in the same direction throughout the period of migration (Haas and Gilmour, 2006; Lecaudey et al., 2008). A lack of coordination in movement among cells within the pLLP disrupts its migration (Haas and Gilmour, 2006; Lecaudey et al., 2008; Valentin et al., 2007). To investigate the cellular basis of the migratory defects in pLLP depleted of Gβ1, we performed higher magnification (20 ×) confocal time-lapse imaging of 30-hpf embryos. The control pLLP displayed an elongated morphology, and a clear polarity characterized by mesenchymal-like cells in the leading region and rosette-like proneuromasts in the trailing region (Fig. 3C) (Lecaudey et al., 2008). Moreover, cells within the pLLP migrated at a similar speed and in the same direction, exhibiting coordinated movement toward the tail (Movie 3), as indicated by the predominantly parallel migration traces in the kymograph (Fig. 3C'). In contrast, the pLLP in Gβ1 morphants displayed poor polarity and the cells within it often changed their direction of migration, as revealed by the "zigzag" pattern of cell traces in the kymograph (Fig. 3D and D'). This migration defect may render the pLLP incapable of migrating coordinately (Movie 4), and is similar to the defect observed in *cxcr4b*$^{(-/-)}$ embryos, which lack the Cxcr4b chemokine receptor (Haas and Gilmour, 2006).

Supplementary material related to this article can be found online at http://dx.doi.org/10.1016/j.ydbio.2013.10.027.

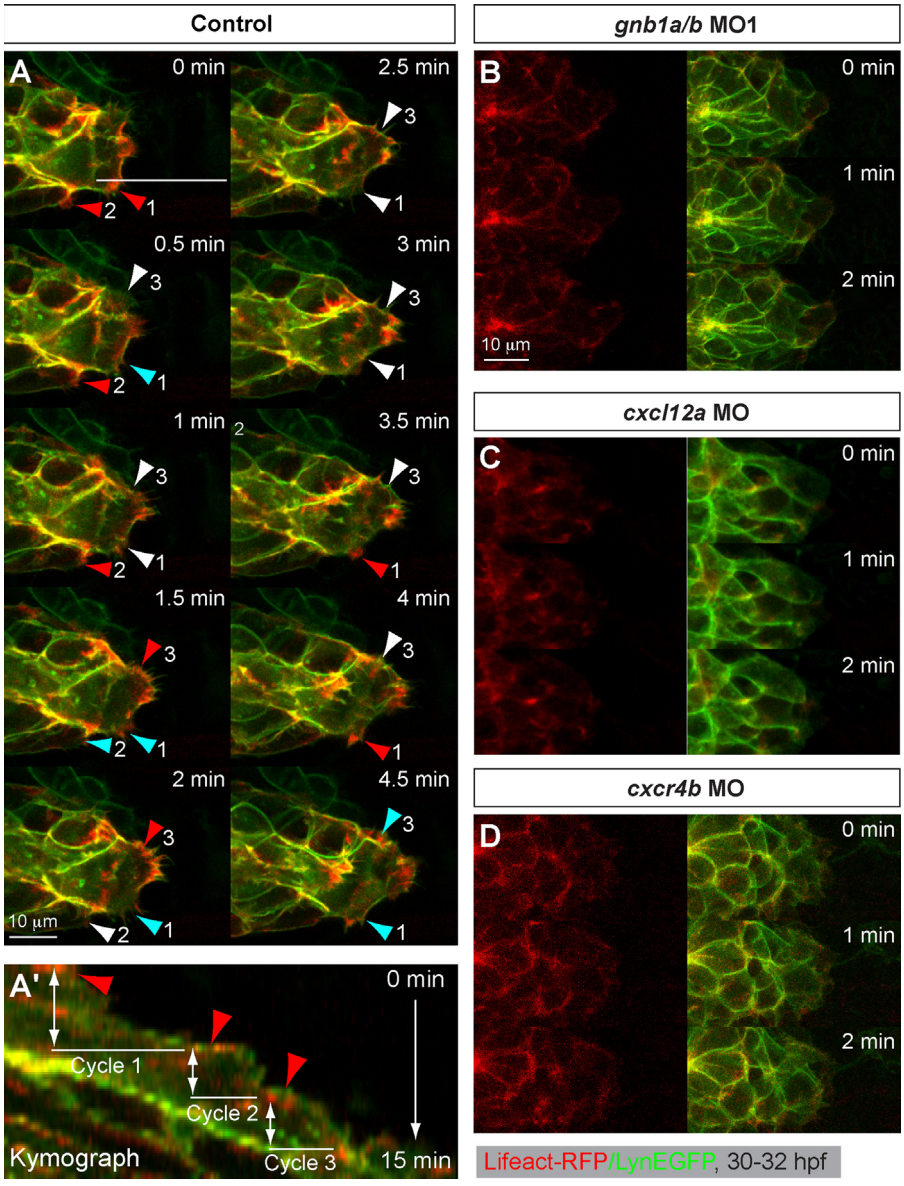

Fig. 6. Gβ1 signaling regulates actin dynamics in the leader cells of the pLLP. Confocal time-lapse movies taken on *Tg(-135bpcxcr4b:lifeact-RFP)*/*Tg(-8.0cldnb:lynEGFP)* double-transgenic embryos at 30–32 hpf, in which actin cytoskeleton dynamics were revealed by Lifeact-RFP labeling, and pLLP cell membrane by membrane-bound EGFP. (A-A') (A) Montage images of the control pLLP leader cells from a 4.5-min confocal time-lapse movie. A few protrusion areas (arrowheads) were highlighted (red: high actin labeling, Cyan: decreased actin labeling, and white: faint or no actin labeling). Numbers follow the same area. A 19.5-min time-lapse recording is shown in Movie 9. (A') The kymograph image was generated from 15-min movie along the line shown in the snapshot at 0 min time point, showing the relative positions of Lifeact-RFP and LynEGFP labeling. A few cycles of association and dissociation of Lifeact-RFP enrichment (arrowheads) with GFP were shown. (B, D) Snapshots of the leading region of the pLLP of *gnb1a*/*b* MO- (B, Movies 10), *cxcl12a* MO- (C) or *cxcr4b* MO- (D) injected embryos.

Gβ1 in the leading region of the pLLP is required for proper migration

A small group of Cxcr4b-expressing cells located at the tip of pLLP, i.e., the leaders cells, organize and spearhead the migration of the entire pLLP in response to chemokine signaling (Haas and Gilmour, 2006). To determine if Gβ1 signaling functions in the Cxcr4b-expressing leader cells to control pLLP migration, we performed genetic mosaic experiments, transplanting rhodamine dextran-labeled wild-type (WT) donor cells into the presumptive placode region of *Tg(-8.0cldnb:lynEGFP)* embryos that had been injected with *gnb1a*/*b* MOs (Fig. 4A). Time-lapse experiments were performed on morphant host embryos in which the pLLP contained transplanted WT cells to evaluate their effects on pLLP migration. Our analyses revealed that all ten embryos in which WT donor cells were present in the leading region of the pLLP, the structure was elongated, exhibited polarity and migrated in a coordinated manner (i.e., yielded parallel cell traces in the kymograph; Fig. 4B–E, Movie 5). Consistent with previous findings (Haas and Gilmour, 2006), even a few WT donor cells in the leading region were sufficient to rescue the migration defect in pLLP deficient for Gβ1 (Fig. 4D, Movie 5). Within individual embryos, the transplanted pLLP migrated to the tip of the tail by 48 hpf (Fig. 4C), whereas the non-transplanted pLLP on the other side of the same embryo failed to migrate properly, stopping at the middle of the trunk (asterisk, Fig. 4B and C). Examination of six embryos in which WT donor cells were present in the trailing region of the pLLP revealed very different outcomes: the defective morphology and migration of the pLLP was not rescued in any of these embryos (Fig. 4F–H, Movie 6). As expected, the WT cells in these embryos were unable to overcome the defects caused by the morphant cells, and displayed uncoordinated cell movements similar to those in non-transplanted Gβ1-deficient embryos

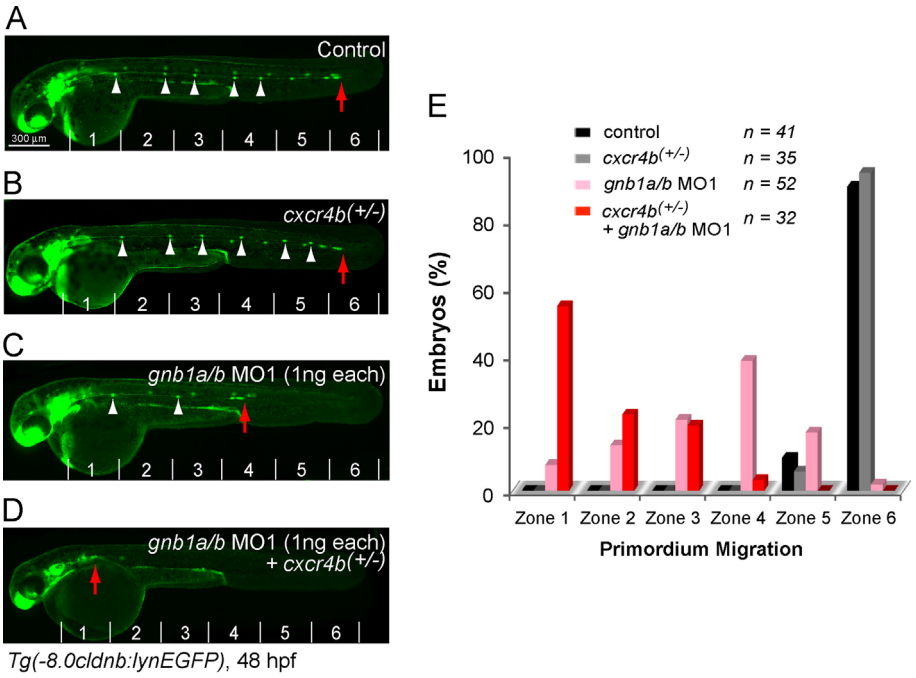

Fig. 7. Gβ1 acts synergistically with Cxcr4b to regulate migration of the pLLP. (A–D) Epifluorescence images of the following 48-hpf *Tg(-8.0cldnb:lynEGFP)* embryos: WT uninjected control (A), *cxcr4b*$^{(+/-)}$ (B), WT injected with a low dose of *gnb1a/b* MO1 (1 ng, C) and *cxcr4b*$^{(+/-)}$ injected with a low dose of *gnb1a/b* MO1 (1 ng, D). Lateral views with anterior to the left; white arrowheads, NMs; and red arrows, posterior-most deposited NM. (F) Quantification of pLLP migration in embryos, as indicated in Fig. 2.

(Fig. 4I, Movie 6). Together, these data suggest that Gβ1 acts in the leader cells to control pLLP migration.

Supplementary material related to this article can be found online at http://dx.doi.org/10.1016/j.ydbio.2013.10.027.

Gβ1 controls pLLP migration by regulating the protrusive activity of the leader cells

Given that Gβ1 functions in the leader cells, we further examined its role in regulating cellular behavior in this region. In WT embryos, the cells at the very tip of the pLLP display prominent filopodia and pseudopodia, suggesting that they migrate actively (Fig. 5A, Movie 7) (Haas and Gilmour, 2006). In *gnb1a/b* morphants, by contrast, the pLLP appeared to be rounded and there were no obvious leading cells at the front (Fig. 5B, Movie 8). Analysis of the cells in the leading region of the morphants revealed that they produced fewer protrusions, and that although they produced filopodia, these were significantly shorter than those in WT pLLP (Fig. 5C and D, $p < 0.05$, student's *t*-test, Movie 8). These results suggest that Gβ1 regulates the protrusive activity of the leader cells in the pLLP.

Supplementary material related to this article can be found online at http://dx.doi.org/10.1016/j.ydbio.2013.10.027.

Actin assembly and remodeling underlie the formation of cell protrusions in migrating cells (Insall and Machesky, 2009; Le Clainche and Carlier, 2008). To determine the role of actin cytoskeleton dynamics in pLLP migration, we generated a stable transgenic line *Tg(-135bpcxcr4b:lifeact-RFP)* in which the filamentous-actin (F-actin) of the pLL cells is labeled with the actin-binding protein Lifeact fused to RFP (Kardash et al., 2010; Riedl et al., 2008) using the *cxcr4b* mini-promoter (Gamba et al., 2010). We used the *Tg(-8.0cldnb:lynEGFP)* strain to generate this line, and found that LifeactRFP is expressed in the migrating pLLP and deposited NMs (Fig. S5A and B). In the doubly transgenic *Tg(-8.0cldnb:lynEGFP)/Tg(-135bpcxcr4b:lifeact-RFP)* embryos, the pLLP migrated at a speed comparable to that in their *Tg(cldnb:lynEGFP)* siblings, and NMs were deposited at regular intervals (Fig. S5A–D). Thus, the expression of Lifeact-RFP in the pLL does not affect either pLLP migration or NM deposition.

We next performed confocal imaging to examine dynamics of the actin cytoskeleton in the migrating pLLP. Consistent with phalloidin staining in fixed samples (Hava et al., 2009), the analysis of Lifeact-RFP indicated that F-actin was highly enriched at central apical points of the rosette structures in the pLLP, as marked by cldnb:lynEGFP (Fig. S5E, arrowheads). This finding supports the idea that apical constriction of the actomyosin network drives rosette formation (Harding and Nechiporuk, 2012; Hava et al., 2009). Additionally, accumulations of Lifeact-RFP signal were prominent at the leading edge of the pLLP (Fig. 6A, red arrowheads and Fig. S5E, arrows). Strikingly, the Lifeact-RFP signal at these sites exhibited cycles of accumulation and dispersion, which we refer as "actin bursts". Detailed analyses of montage images generated from time-lapse movies collected at 30-s intervals revealed that F-actin accumulated to high levels in protrusions as they formed and extended, disappeared once they stopped expanding and began to retract, and then reappeared where new protrusions emerged in the next cycle (Fig. 6A, Movie 9). This cyclic actin accumulation phenomenon is supported by kymograph analyses, which showed that F-actin was highly enriched as protrusions emerged and diminished once they had reached their maximal length (Fig. 6A'). This cyclic pattern of actin bursts may reflect the dynamic processes of actin assembly and disassembly. Together these findings suggest that actin bursts are involved in promoting the formation of membrane protrusions, and thus pLLP migration. Notably, no actin bursts were observed in the cells within rosette structures (Movie 9), suggesting that pLLP migration is empowered by rapid actin polymerization and depolymerization at the leading front. Consistent with the stalled pLLP migration in embryos defective for Gβ1, actin bursts were completely absent at the leading edge of the morphant pLLP; only a weak and transient F-actin signal was observed in this region (Fig. 6B, Movie 10). However, in pLLP defective for Gβ1 signaling, F-actin accumulation in the rosette centers was not affected (Movie 10, Fig. S6), and the average LifeactRFP intensity of cells

in the trailing region was comparable to that in controls (Fig. S6). Our data indicate that Gβ1 signaling is required specifically to promote actin dynamics within the leader cells, and thus for pLLP migration. Similar defects in actin dynamics were also found in the pLLP of embryos defective for Cxcl12a or Cxcr4b (Fig. 6C and D), further supporting the notion that chemokine signaling controls dynamics of the actin cytoskeleton, probably through a Gβ1-dependent pathway.

Supplementary material related to this article can be found online at http://dx.doi.org/10.1016/j.ydbio.2013.10.027.

Gβ1 and Cxcr4b act synergistically to regulate pLLP migration

The striking phenotypic similarities between embryos depleted of Gβ1 and those deficient for Cxcl12a chemokine signaling suggest that these proteins function in the same genetic pathway. To determine if Cxcr4b and Gβ1 interact genetically, we performed a synergy experiment, assessing their combined effects on pLLP migration. We injected *Tg*(*-8.0cldnb:lynEGFP*) embryos and embryos derived from crosses between *Tg*(*-8.0cldnb:lynEGFP*) and *cxcr4b*$^{(-/-)}$ homozygous fish with a low dose of *gnb1a*/*b* MO1 (1 ng each). Such MO injection in control *Tg*(*-8.0cldnb:lynEGFP*) embryos caused mild pLLP migration defects, with a majority of the pLLP migrating to the middle of the trunk by 48 hpf (Fig. 7C and E). In the heterozygous *cxcr4b*$^{(+/-)}$ mutant embryos, pLLP migration and NM deposition were normal (Fig. 7B and E). The heterozygous *cxcr4b*$^{(+/-)}$ mutant embryos injected with the same amount of MO, however, exhibited significantly stronger pLLP migration defects: by 48 hpf, 55% of the pLLP had migrated only to zone 1, and 23% to zone 2 (Fig. 7D and E, $p<0.05$ compared to partial inhibition group, Chi-Square test). These defects were similar to those observed in *cxcr4b*$^{(-/-)}$ embryos, and in embryos injected with a high dose of *gnb1a*/*b* MO1 (compare Fig. 7D with Fig. 2D). These findings suggest that Gβ1 and Cxcr4b interact genetically, and that they act synergistically to regulate pLLP migration.

Discussion

Gβ1 probably functions downstream of the Cxcl12a/Cxcr4b signaling axis to regulate pLLP migration

In this study, we have identified an essential role for Gβ1 in regulating collective migration of the zebrafish pLLP. We show that pLLP migration is severely impaired in embryos defective for Gβ1 (Figs. 2 and S1). It has been reported that the increased apoptosis associated with the general toxicity of MOs can affect LL development, however, this non-specific effect of MOs typically leads to a reduction in the frequency of NM deposition rather than to stalled pLLP migration. In addition, several aspects of the current study support the notion that apoptosis is not a concern. Firstly, we coinjected the embryos with a MO targeting *p53* to reduce the possibility of apoptosis (Robu et al., 2007). Secondly, the pLLP migration defects observed in embryos injected with different combinations of two independent sets of previously validated MOs targeting the two Gβ1 isoforms were similar (Figs. 1 and S2). Thirdly, our prolonged time-lapse movies did not show obvious dying cells in migrating pLLP of control and MO-injected embryos (Movies 1 and 2). Lastly, TUNEL analysis showed no excessive cell apoptosis within Gβ1-depleted pLLP. Thus, we are confident that the severe disruption of pLLP migration we observed in embryos deficient for Gβ1 is unlikely due to cell death, but rather to the inhibition of Gβ1 expression.

Our analysis also suggest that Gβ1 functions downstream of Cxcl12a/Cxcr4b to control pLLP migration. Time-lapse imagining revealed that the migration of Gβ1-deficient pLLP initiated, but was slow and stopped prematurely, due to uncoordinated movements among pLLP cells (Figs. 2 and 3, Movies 1–4). Furthermore, genetic mosaic experiments demonstrated that coordinated and directed pLLP migration requires Gβ1 signaling within the leader cells of the pLLP (Fig. 4, Movies 5 and 6). Such impaired pLLP migration in the context of the Gβ1 deficiency, and a requirement for Gβ1 in the leader cells of the pLLP, are reminiscent of the phenotypes in embryos deficient for signaling by the chemokine Cxcl12a/Cxcr4b/Cxcr7 axis (Dambly-Chaudiere et al., 2007; David et al., 2002; Haas and Gilmour, 2006; Li et al., 2004; Valentin et al., 2007). However, the expression patterns of *cxcl12a*, *cxcr4b* and *cxcr7* were not affected in embryos defective for Gβ1 (Fig. S4). Given that the Gβγ dimer transmits Cxcr4b signal in regulating the chemotaxis of many other cell types (Peracino et al., 1998; Rickert et al., 2000), we propose that Cxcr4b also functions through Gβγ to regulate pLLP migration. Our discovery that the leader cells of Gβ1-deficient pLLP lost protrusive activity (Figs. 5 and 6, Movies 7 and 8) suggests that they do not respond to the chemoattractant Cxcl12a. Furthermore, the fact that we observed striking actin dynamics, i.e. “actin bursts,” in the leader cells of the normal pLLP but not in pLLP defective for Gβ1, Cxcr4b or Cxcl12a (Fig. 6, Movies 9 and 10) indicates that the dynamic actin turnover is critical for pLLP migration, which is controlled by chemokine and Gβ1 signaling. Finally, our findings that Gβ1 and Cxcr4b act synergistically in regulating pLLP migration also support the hypothesis that Gβ1 functions downstream of Cxcl12a/Cxcr4b to control pLLP migration. Nevertheless, we cannot exclude the possibility that Gβ1 functions in a parallel pathway to regulate pLLP migration.

Specific functions of Gβ1 in pLLP migration

Gβγ subunits are central to signal transduction by GPCRs (Dupre et al., 2009; Khan et al., 2013; Smrcka, 2008). Five distinct Gβ and 12 Gγ subunit genes have been identified in mammals. With the exception of Gβ5, the Gβ proteins share 79–98% amino acid sequence similarity. The Gγ subunits are more diverse, with 25–76% amino acid sequence similarity. It has been shown that different Gβ and Gγ isoforms can pair to form distinct Gβγ complexes, and these may interact with different Gα isoforms to form distinct heterotrimeric G protein complexes that couple to particular GPCRs to transmit specific cellular signals. For example, although both Gβ1 and Gβ2 are expressed in the mouse macrophage cell line J774A.1, C5a-stimulated chemotaxis of these cells is mediated primarily by Gβ2 (Hwang et al., 2004). Similarly, Gβ1 and Gβ2 have been shown to play distinct roles in regulating the chemotaxis of primary mouse neutrophils, and in bacterial phagocytosis and killing (Zhang et al., 2010). Our previous studies have shown that, as is the case for mammals, five Gβ isoforms are expressed in zebrafish (Xu et al., 2012). However, given that only Gβ1 and Gβ4 are expressed in the LL, the others are unlikely to be involved in pLLP function. Intriguingly, despite the fact that Gβ4 is also expressed in the LL, only Gβ1 contributes to the regulation of pLLP migration. One study had reported that Gβ1 is involved in regulating cardiac contractility in zebrafish, but had not assessed the role of Gβ4 (Hippe et al., 2009). The reason for the difference in involvement of Gβ1 and Gβ4 in pLLP migration is not clear. It is unlikely due to differences in expression in distinct cell types within the pLLP because Gβ1 and Gβ4 transcripts were detected throughout the pLLP cell population (Figs. 1 and S1B and C). Nevertheless, we cannot exclude the possibility that Gβ1 and Gβ4 may be located in different subcellular compartments. Given that inhibition of Gβ1 and Gβ4 led to similar decreases in the expression of total Gβ in the pLLP, as detected by immunofluorescence staining, the two proteins are thought to be expressed at similar levels in this tissue (Fig. S1C). Therefore, differences in the expression levels of the two proteins are also unlikely to account

for their different functions in pLLP migration. Similar to their mammalian counterparts, zebrafish Gβ1 and Gβ4 share 90% amino acid sequence identity and 96% similarity (Xu et al., 2012). Nevertheless, they may form distinct heterotrimeric complexes with different Gγ and Gα subunits, and thus exhibit different affinities for particular GPCRs in specific tissues. Consistent with this notion, we found that embryos depleted of Gβ4 but not Gβ1 exhibited other abnormities including an excess of otoliths, a ventrally curved axis and kidney cysts (Fig. 2E and not shown), phenotypes that are frequently observed when ciliated epithelia are defective (Panizzi et al., 2007). Together, these data highlight the functional differences among Gβ isoforms in regulating specific developmental processes of different tissues *in vivo*.

Possible roles of chemokine/G protein signaling in regulating collective cell migration

Despite the discovery of Cxcl12a chemokine and its cognate receptors Cxcr4b and Cxcr7 are key regulators of pLLP migration, the underlying signaling mechanisms are still largely unknown (Gallardo et al., 2010). Thus, our findings on the involvement of Gβ1-mediated signaling in pLLP migration represent an important step towards understanding the molecular mechanisms that regulate this process. Based on the well-defined role that Gβγ plays in mediating the function of chemokine receptors in leukocytes, we propose that Gβ1 mediates pLLP migration by activating downstream effectors through Gβγ. Gβγ has been shown to activate diverse effectors, including PI3K, PLC and MAPKs to control cell migration (Dupre et al., 2009; Khan et al., 2013). Moreover, Gβγ may activate RhoGTPases through RhoGEFs to facilitate organization of the actin cytoskeleton for cell polarization and directional migration (Andrews et al., 2007; Wang, 2009). We have shown previously that Gβγ regulates PGC migration by controlling the Rac activation (Xu et al., 2012), and that Rac activation is sufficient to direct and organize the migration of neutrophils (as single cells) (Yoo et al., 2010) and border cells (as collective cells) (Wang et al., 2010). Thus, in the future it will be important to determine if Gβ1 transmits chemotactic signals from Cxcr4b to Rac to control arrangement of the actin cytoskeleton in leader cells during pLLP migration.

Collective cell migration is a feature necessary for the dissemination of many types of cancer to distant organs (Friedl et al., 2004, 2012). In some cases, leader cells have been found to direct the migration of cohorts of invasive cancer cells (Gaggioli et al., 2007; Wolf et al., 2007). Notably, aberrant activation of the Cxcl12/Cxcr4b signaling axis has been implicated in tumor metastasis (Balkwill, 2004; Kulbe et al., 2004), and our recent studies indicate that Gβγ transmits signals from various GPCRs, including Cxcr4, to promote the metastasis of breast cancer in nude mice (Tang et al., 2011). Given our findings that Gβ1 mediates the function of Cxcr4b in controlling leader-cell migration in the pLLP, we will be interested in determining if a similar mechanism is employed by the leader cells to direct cancer metastasis.

In summary, our studies reveal a specific role for Gβ1 signaling in regulating collective cell migration of the zebrafish pLLP. We show that of the two major Gβ isoforms expressed in the pLLP, Gβ1, but not Gβ4, functions in the leader cells, probably downstream of Cxcl12a/Cxcr4b signaling. Furthermore, we demonstrate that Cxcl12a/Cxcr4b/Gβ1 signaling is critical for regulating dynamics of the actin cytoskeleton to promote pLLP migration. Our findings represent *in vivo* evidence for functional differences of Gβ1 and Gβ4 in regulating pLLP migration. Moreover, our study has significant implications for understanding the mechanisms underlying collective migration—a process vital to both normal development and cancer dispersion.

Acknowledgments

This study is supported by Grants: NIH/NCRR K99R00RR024119 and AHA12GRNT11670009 (to FL); AHA10GRNT3620015 and NIH R01GM094255 (to SC). We thank Laurent Gamba and Christine Dambly-Chaudière (Universite Montpellier II, France) for providing the 139 bp *cxcr4b* promoter, and Kacey Mersch, Xiaoyun Tang, Zhizeng Sun and Catherine Wang for technical support.

Appendix A. Supplementary material

Supplementary data associated with this article can be found in the online version at http://dx.doi.org/10.1016/j.ydbio.2013.10.027.

References

Aman, A., Nguyen, M., Piotrowski, T., 2011. Wnt/β-catenin dependent cell proliferation underlies segmented lateral line morphogenesis. Dev. Biol. 349, 470–482.
Aman, A., Piotrowski, T., 2008. Wnt/β-catenin and Fgf signaling control collective cell migration by restricting chemokine receptor expression. Dev. Cell 15, 749–761.
Aman, A., Piotrowski, T., 2009. Multiple signaling interactions coordinate collective cell migration of the posterior lateral line primordium. Cell Adhes. Migr. 3, 365–368.
Andrews, S., Stephens, L.R., Hawkins, P.T., 2007. PI3K class IB pathway in neutrophils. Sci. STKE 2007, cm3.
Balkwill, F., 2004. Cancer and the chemokine network. Nat. Rev. Cancer 4, 540–550.
Behra, M., Bradsher, J., Sougrat, R., Gallardo, V., Allende, M.L., Burgess, S.M., 2009. Phoenix is required for mechanosensory hair cell regeneration in the zebrafish lateral line. PLoS Genet. 5, e1000455.
Berepiki, A., Lichius, A., Shoji, J.Y., Tilsner, J., Read, N.D., 2010. F-actin dynamics in *Neurospora crassa*. Eukaryot. Cell 9, 547–557.
Caussinus, E., Colombelli, J., Affolter, M., 2008. Tip-cell migration controls stalk-cell intercalation during Drosophila tracheal tube elongation. Curr. Biol. 18, 1727–1734.
Dambly-Chaudiere, C., Cubedo, N., Ghysen, A., 2007. Control of cell migration in the development of the posterior lateral line: antagonistic interactions between the chemokine receptors CXCR4 and CXCR7/RDC1. BMC Dev. Biol. 7, 23.
Dambly-Chaudiere, C., Sapede, D., Soubiran, F., Decorde, K., Gompel, N., Ghysen, A., 2003. The lateral line of zebrafish: a model system for the analysis of morphogenesis and neural development in vertebrates. Biol. Cell 95, 579–587.
David, N.B., Sapede, D., Saint-Etienne, L., Thisse, C., Thisse, B., Dambly-Chaudiere, C., Rosa, F.M., Ghysen, A., 2002. Molecular basis of cell migration in the fish lateral line: role of the chemokine receptor CXCR4 and of its ligand, SDF1. Proc. Natl. Acad. Sci. USA 99, 16297–16302.
De Smet, F., Segura, I., De Bock, K., Hohensinner, P.J., Carmeliet, P., 2009. Mechanisms of vessel branching: filopodia on endothelial tip cells lead the way. Arterioscler. Thromb. Vasc. Biol. 29, 639–649.
Doitsidou, M., Reichman-Fried, M., Stebler, J., Koprunner, M., Dorries, J., Meyer, D., Esguerra, C.V., Leung, T., Raz, E., 2002. Guidance of primordial germ cell migration by the chemokine SDF-1. Cell 111, 647–659.
Dupre, D.J., Robitaille, M., Rebois, R.V., Hebert, T.E., 2009. The role of Gbetagamma subunits in the organization, assembly, and function of GPCR signaling complexes. Annu. Rev. Pharmacol. Toxicol. 49, 31–56.
Friedl, P., Gilmour, D., 2009. Collective cell migration in morphogenesis, regeneration and cancer. Nat. Rev. Mol. Cell Biol. 10, 445–457.
Friedl, P., Hegerfeldt, Y., Tusch, M., 2004. Collective cell migration in morphogenesis and cancer. Int. J. Dev. Biol. 48, 441–449.
Friedl, P., Locker, J., Sahai, E., Segall, J.E., 2012. Classifying collective cancer cell invasion. Nat. Cell Biol. 14, 777–783.
Gaggioli, C., Hooper, S., Hidalgo-Carcedo, C., Grosse, R., Marshall, J.F., Harrington, K., Sahai, E., 2007. Fibroblast-led collective invasion of carcinoma cells with differing roles for RhoGTPases in leading and following cells. Nat. Cell Biol. 9, 1392–1400.
Gallardo, V.E., Liang, J., Behra, M., Elkahloun, A., Villablanca, E.J., Russo, V., Allende, M.L., Burgess, S.M., 2010. Molecular dissection of the migrating posterior lateral line primordium during early development in zebrafish. BMC Dev. Biol. 10, 120.
Gamba, L., Cubedo, N., Ghysen, A., Lutfalla, G., Dambly-Chaudiere, C., 2010. Estrogen receptor ESR1 controls cell migration by repressing chemokine receptor CXCR4 in the zebrafish posterior lateral line system. Proc. Natl. Acad. Sci. USA 107, 6358–6363.
Ghysen, A., Dambly-Chaudiere, C., 2004. Development of the zebrafish lateral line. Curr. Opin. Neurobiol. 14, 67–73.
Ghysen, A., Dambly-Chaudiere, C., 2007. The lateral line microcosmos. Genes Dev. 21, 2118–2130.
Haas, P., Gilmour, D., 2006. Chemokine signaling mediates self-organizing tissue migration in the zebrafish lateral line. Dev. Cell 10, 673–680.
Harding, M.J., Nechiporuk, A.V., 2012. Fgfr-Ras-MAPK signaling is required for apical constriction via apical positioning of Rho-associated kinase during mechanosensory organ formation. Development 139, 3130–3135.

Hava, D., Forster, U., Matsuda, M., Cui, S., Link, B.A., Eichhorst, J., Wiesner, B., Chitnis, A., Abdelilah-Seyfried, S., 2009. Apical membrane maturation and cellular rosette formation during morphogenesis of the zebrafish lateral line. J. Cell Sci. 122, 687–695.

Hippe, H.J., Wolf, N.M., Abu-Taha, I., Mehringer, R., Just, S., Lutz, S., Niroomand, F., Postel, E.H., Katus, H.A., Rottbauer, W., et al., 2009. The interaction of nucleoside diphosphate kinase B with Gbetagamma dimers controls heterotrimeric G protein function. Proc. Natl. Acad. Sci. USA 106, 16269–16274.

Hwang, J.I., Fraser, I.D., Choi, S., Qin, X.F., Simon, M.I., 2004. Analysis of C5a-mediated chemotaxis by lentiviral delivery of small interfering RNA. Proc. Natl. Acad. Sci. USA 101, 488–493.

Insall, R.H., Machesky, L.M., 2009. Actin dynamics at the leading edge: from simple machinery to complex networks. Dev. Cell 17, 310–322.

Kardash, E., Reichman-Fried, M., Maitre, J.L., Boldajipour, B., Papusheva, E., Messerschmidt, E.M., Heisenberg, C.P., Raz, E., 2010. A role for Rho GTPases and cell-cell adhesion in single-cell motility in vivo. Nat. Cell Biol. 12, 47–53. (sup pp. 1–11).

Khan, S.M., Sleno, R., Gora, S., Zylbergold, P., Laverdure, J.P., Labbe, J.C., Miller, G.J., Hebert, T.E., 2013. The expanding roles of Gβγ subunits in G protein-coupled receptor signaling and drug action. Pharmacol. Rev. 65, 545–577.

Kimmel, C.B., Ballard, W.W., Kimmel, S.R., Ullmann, B., Schilling, T.F., 1995. Stages of embryonic development of the zebrafish. Dev. Dyn. 203, 253–310.

Knaut, H., Werz, C., Geisler, R., Nusslein-Volhard, C., 2003. A zebrafish homologue of the chemokine receptor Cxcr4 is a germ-cell guidance receptor. Nature 421, 279–282.

Kozlowski, D.J., Whitfield, T.T., Hukriede, N.A., Lam, W.K., Weinberg, E.S., 2005. The zebrafish dog-eared mutation disrupts eya1, a gene required for cell survival and differentiation in the inner ear and lateral line. Dev. Biol. 277, 27–41.

Kulbe, H., Levinson, N.R., Balkwill, F., Wilson, J.L., 2004. The chemokine network in cancer—much more than directing cell movement. Int. J. Dev. Biol. 48, 489–496.

Kwan, K.M., Fujimoto, E., Grabher, C., Mangum, B.D., Hardy, M.E., Campbell, D.S., Parant, J.M., Yost, H.J., Kanki, J.P., Chien, C.B., 2007. The Tol2kit: a multisite gateway-based construction kit for Tol2 transposon transgenesis constructs. Dev. Dyn. 236, 3088–3099.

Le Clainche, C., Carlier, M.F., 2008. Regulation of actin assembly associated with protrusion and adhesion in cell migration. Physiol. Rev. 88, 489–513.

Lecaudey, V., Cakan-Akdogan, G., Norton, W.H., Gilmour, D., 2008. Dynamic Fgf signaling couples morphogenesis and migration in the zebrafish lateral line primordium. Development 135, 2695–2705.

Lecaudey, V., Gilmour, D., 2006. Organizing moving groups during morphogenesis. Curr. Opin. Cell Biol. 18, 102–107.

Li, Q., Shirabe, K., Kuwada, J.Y., 2004. Chemokine signaling regulates sensory cell migration in zebrafish. Dev. Biol. 269, 123–136.

Lin, F., Chen, S., Sepich, D.S., Panizzi, J.R., Clendenon, S.G., Marrs, J.A., Hamm, H.E., Solnica-Krezel, L., 2009. Gα12/13 regulate epiboly by inhibiting E-cadherin activity and modulating the actin cytoskeleton. J. Cell Biol. 184, 909–921.

Lin, F., Sepich, D.S., Chen, S., Topczewski, J., Yin, C., Solnica-Krezel, L., Hamm, H., 2005. Essential roles of Gα12/13 signaling in distinct cell behaviors driving zebrafish convergence and extension gastrulation movements. J. Cell Biol. 169, 777–787.

Ma, E.Y., Raible, D.W., 2009. Signaling pathways regulating zebrafish lateral line development. Curr. Biol. 19, R381–386.

Nechiporuk, A., Raible, D.W., 2008. FGF-dependent mechanosensory organ patterning in zebrafish. Science 320, 1774–1777.

Nica, G., Herzog, W., Sonntag, C., Nowak, M., Schwarz, H., Zapata, A.G., Hammerschmidt, M., 2006. Eya1 is required for lineage-specific differentiation, but not for cell survival in the zebrafish adenohypophysis. Dev. Biol. 292, 189–204.

Panizzi, J.R., Jessen, J.R., Drummond, I.A., Solnica-Krezel, L., 2007. New functions for a vertebrate Rho guanine nucleotide exchange factor in ciliated epithelia. Development 134, 921–931.

Parinov, S., Kondrichin, I., Korzh, V., Emelyanov, A., 2004. Tol2transposon-mediated enhancer trap to identify developmentally regulated zebrafish genes *in vivo*. Dev. Dyn. 231, 449–459.

Peracino, B., Borleis, J., Jin, T., Westphal, M., Schwartz, J.M., Wu, L., Bracco, E., Gerisch, G., Devreotes, P., Bozzaro, S., 1998. G protein β subunit-null mutants are impaired in phagocytosis and chemotaxis due to inappropriate regulation of the actin cytoskeleton. J. Cell Biol. 141, 1529–1537.

Rickert, P., Weiner, O.D., Wang, F., Bourne, H.R., Servant, G., 2000. Leukocytes navigate by compass: roles of PI3Kγ and its lipid products. Trends Cell Biol. 10, 466–473.

Riedl, J., Crevenna, A.H., Kessenbrock, K., Yu, J.H., Neukirchen, D., Bista, M., Bradke, F., Jenne, D., Holak, T.A., Werb, Z., et al., 2008. Lifeact: a versatile marker to visualize F-actin. Nat. Methods 5, 605–607.

Robu, M.E., Larson, J.D., Nasevicius, A., Beiraghi, S., Brenner, C., Farber, S.A., Ekker, S.C., 2007. p53 activation by knockdown technologies. PLoS Genet. 3, e78.

Rorth, P., 2009. Collective cell migration. Annu. Rev. Cell Dev. Biol. 25, 407–429.

Smrcka, A.V., 2008. G protein βγ subunits: central mediators of G protein-coupled receptor signaling. Cell Mol. Life Sci. 65, 2191–2214.

Tang, X., Sun, Z., Runne, C., Madsen, J., Domann, F., Henry, M., Lin, F., Chen, S., 2011. A critical role of Gβγ in tumorigenesis and metastasis of breast cancer. J. Biol. Chem. 286, 13244–13254.

Thelen, M., 2001. Dancing to the tune of chemokines. Nat. Immunol. 2, 129–134.

Thisse, B., Thisse, C., 2004. Fast release clones: a high throughput expression analysis. ZFIN Direct Data Submission ⟨http://zfin.org⟩.

Thisse, C., Thisse, B., 2008. High-resolution in situ hybridization to whole-mount zebrafish embryos. Nat. Protoc. 3, 59–69.

Valentin, G., Haas, P., Gilmour, D., 2007. The chemokine SDF1a coordinates tissue migration through the spatially restricted activation of Cxcr7 and Cxcr4b. Curr. Biol. 17, 1026–1031.

Wang, F., 2009. The signaling mechanisms underlying cell polarity and chemotaxis. Cold Spring Harbor Perspect. Biol. 1, a002980.

Wang, X., He, L., Wu, Y.I., Hahn, K.M., Montell, D.J., 2010. Light-mediated activation reveals a key role for Rac in collective guidance of cell movement in vivo. Nat. Cell Biol. 12, 591–597.

Wolf, K., Wu, Y.I., Liu, Y., Geiger, J., Tam, E., Overall, C., Stack, M.S., Friedl, P., 2007. Multi-step pericellular proteolysis controls the transition from individual to collective cancer cell invasion. Nat. Cell Biol. 9, 893–904.

Xu, H., Echemendia, N., Chen, S., Lin, F., 2011. Identification and expression patterns of members of the protease-activated receptor (PAR) gene family during zebrafish development. Dev. Dyn. 240, 278–287.

Xu, H., Kardash, E., Chen, S., Raz, E., Lin, F., 2012. Gβγ signaling controls the polarization of zebrafish primordial germ cells by regulating Rac activity. Development 139, 57–62.

Yoo, S.K., Deng, Q., Cavnar, P.J., Wu, Y.I., Hahn, K.M., Huttenlocher, A., 2010. Differential regulation of protrusion and polarity by PI3K during neutrophil motility in live zebrafish. Dev. Cell 18, 226–236.

Zhang, Y., Tang, W., Jones, M.C., Xu, W., Halene, S., Wu, D., 2010. Different roles of G protein subunits β1 and β2 in neutrophil function revealed by gene expression silencing in primary mouse neutrophils. J. Biol. Chem. 285, 24805–24814.